JOURNAL OF OPTOELECTRONICS AND ADVANCED MATERIALS Vol. 8, No. 1, Febraury 2006, p. 339 - 344

Contribution to the cavity model for analysis of microstrip patch antennas

D. D. SANDU*, O. G. AVADANEI, A. IOACHIM[a], D. IONESI[b]
Faculty of Physics, University "Al. I. Cuza" of Iaşi, Romania
[a]*National Inst. of Material Physics, P. O. Box MG 7, Bucharest,Romania*
[B]*FERA Bacău, Romania*

In this communication we propose a further improvement of the cavity model for microstrip antennas, given by Richards et al. [1]. The main attention is paid to the calculation of the radiated fields E_θ, E_φ and to the variation of the input impedance as a function of the frequency and the feed point. In our model we have suppose that the magnetic walls are not perfect and the patch acts as a cavity with the length corresponding to its resonance frequency. The validity of the proposed model was proved by comparison of theoretical computations and experimental results.

(Received September 13, 2005; accepted January 26, 2006)

Keywords: Microwaves, Microstrip, Patch antennas, Impedance, Radiation pattern

1. Introduction

During the design procedure of patch antennas there are two important features: the calculation of the radiation pattern for a single patch and for an array; determination of the input impedance that can assure a good matching of the feed line with the patch. In this aspect were proposed many models. In this communication we deal mainly with the improved cavity model given by W. F. Richards et al. [1], which is related to the classical cavity model developed by Y. T. Lo et al. [2]. Besides these models other approaches are known in the literature; among these we can mention: the vector potential approach [3], the dyadic Green's function model [4], the wire grid model [5], and the transmission line model [6,7].

2. General relations for the classical cavity model

The "Classical Cavity Model" [2] is based on the following considerations:

a) The close proximity between the microstrip patch and the ground plane suggest that $\vec{E}$ has only *z* component and $\vec{H}$ has only *xy*-components in the region bounded by the microstrip and ground plane.

b) The fields are independent of the *z*-coordinate for all frequencies of interest.

c) The electric current in the microstrip must have no component normal to the edge at any point on the edge, implying a negligible tangent component of the $\vec{H}$ along the edge.

Thus the region between the patch and ground plane may be treated as a cavity bounded by electric walls above and below, and magnetic walls along the edges. The fields inside the antenna are assumed to be the fields inside of this cavity.

In Fig. 1 we present a rectangular patch of width *a* and length *b* over a ground plane with a dielectric substrate of thickness *h* and the relative permittivity ε_r. Inside this cavity the *z*-directed electric field satisfy the equation

$$\left(\nabla^2 + k_{mnp}^2\right) E_z = j\omega\mu J_e \hat{z} \tag{1}$$

where ∇^2 is the laplacian and J_e is the excitation current. The solution of the homogeneous wave equation for TM_{mnp} mode is given by [8]:

$$E_z = E_0 \cos(k_m x)\cos(k_n y)\cos(k_p z) \tag{2}$$

where E_0 is an amplitude coefficient depending on the excitation condition; the eigenvalues satisfy the equation

$$k_{mnp}^2 = \omega_{mnp}^2 \mu\varepsilon = k_m^2 + k_n^2 + k_p^2 \tag{3}$$

where for a non radiating cavity

$$k_m = m\pi / a, \quad k_n = n\pi / b, \quad k_p = p\pi / h; \tag{4}$$

ε is the permittivity of the substrate and μ its permeability.

Tacking into account the small thickness of the substrate, *p* must be zero for usually frequencies and in this case E_x, E_y, are zero and the magnetic fields components are:

$$H_x = \frac{j\omega\varepsilon}{k_{mnp}^2} k_n E_0 \cos(k_m x)\sin(k_n y)\cos(k_p z)$$

$$H_y = \frac{j\omega\varepsilon}{k_{mnp}^2} k_m E_0 \sin(k_m x)\cos(k_n y)\cos(k_p z) \tag{5}$$

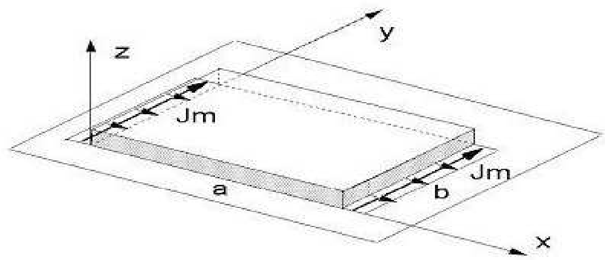

Fig. 1. The representation of radiating currents.

The cavity model assumes that the field structure in the patch antenna is essentially the same as that in the cavity. With those fields we calculate the currents generated by the field E_z, on the side walls:

$$\vec{J}_{my} = E_z \hat{z} \times \hat{x} = E_0 \cos(n\pi y / b)\hat{y} \quad \text{for } x = 0 \text{ and } x = a \tag{6}$$
$$\vec{J}_{mx} = E_z \hat{z} \times \hat{y} = \pm E_0 \cos(m\pi x / a)\hat{x} \quad \text{for } y = 0 \text{ and } b$$

where $\hat{x}, \hat{y}, \hat{z}$ are unity vectors.

In this model only the electric fields generates radiating currents because the magnetic fields are zero at the lateral walls.

For the oscillation mode TM_{100} the currents J_{my} on the walls, $x=0$ and $x=a$, are radiating only; the other two J_{mx} currents on the walls $y=0$ and $y=b$ are nonradiating.

The input conductance is give by the following relation [2]

$$G = \frac{P_r + P_d}{|V|^2} \tag{7}$$

where P_r is the radiated power, P_d is the power lost in dielectric, and V is the voltage at the feeding point.

3. Further improvements of the cavity model

For the real case of a patch excited by a coaxial feed line the field is a superposition of all TM_{mn} modes and therefore the z-directed electric field will be

$$\vec{E}_z(x,y) = \sum_m \sum_n A_{mn}\, \vec{e}_{mn}(x,y) \tag{8}$$

where A_{mn} are the mode amplitude coefficient and $\vec{e}_{mn}$ are the *z*-directed orthonormalized electric field mode vectors. For the elementary case of a nonradiating cavity with perfect open-circuits walls, we have [9]

$$e_{mn}(x,y) = \frac{\chi_{mn}}{\sqrt{\varepsilon abh}} \cos(k_m x)\cos(k_n y) \tag{9}$$

with

$$\chi_{mn} = \begin{cases} 1, & m = 0 \text{ and } n = 0 \\ \sqrt{2} & m = 0 \text{ or } n = 0 \\ 2 & m \neq 0 \text{ and } n \neq 0 \end{cases}$$

If the excitation current J_0 is a *z*-directed current probe I_0 of small rectangular cross-section (d_x, d_y) at the point (x_0, y_0) and zero elsewhere the mode amplitude coefficient is

$$A_{mn} = j I_0 \sqrt{\frac{\mu h}{ab}} \frac{k\chi_{mn}}{k^2 - k_{mn}^2} G_{mn} \cos(k_m x_0)\cos(k_n y_0) \tag{10}$$

where

$$G_{mn} = \frac{\sin(m\pi d_x / 2a)}{m\pi d_x / 2a} \cdot \frac{\sin(n\pi d_y / 2b)}{n\pi d_y / 2b}$$

k is the wave number and k_{mn} is the k_{mnp} for $p=0$.

The factor G_{mn} accounts for the width of the feed, (dx, dy) which, for a coaxial line feeding is five times greater than the physical dimension of the excitation cable [1]. Substituting (10) into (9) we obtain

$$E_z = j I_0 Z_0 k \sum_{m=0}^{\infty} \sum_{n=0}^{\infty} \frac{\psi_{mn}(x,y)\psi_{mn}(x_0,y_0)}{k^2 - k_{mn}^2} G_{mn} \tag{11}$$

where $Z_0 = \sqrt{\mu / \varepsilon}$, $k = \omega\sqrt{\mu\varepsilon}$ and

$$\psi_{mn} = \frac{\chi_{mn}}{\sqrt{ab}} \cos k_m x \cos k_n y \tag{12}$$

Tacking into account that the voltage at the feed point is $V_{in} = -hE_z(x_0, y_0)$ Richards et al. [1] proposed for the input impedance the relation

$$Z_{in} = \frac{V_{in}}{I_0} = -jZ_0 kh \sum_{m=0}^{\infty} \sum_{n=0}^{\infty} \frac{\psi_{mn}^2(x_0,y_0)}{k^2 - k_{mn}^2} G_{mn} \tag{13}$$

But according (13) with k real the impedance would be purely imaginary, and that is in contradiction with experiment. To solve this problem Richards et al. lump all losses into a single “effective dielectric loss” with effective tangent loss δ_{eff}. In this case the wavenumber k would be replaced by an effective wavenumber $k_{eff} = \sqrt{\varepsilon_r(1 - j\delta_{eff})}k_0$. In an ideal cavity $\delta=1/Q$, where Q is the quality factor, therefore

$$\delta_{eff} = P_l / (2\omega W_c) \tag{14}$$

where $P_l=P_r+P_d+P_m$ are the total losses, P_r is the power lost by radiation, P_d is the power lost in dielectric, P_m the power lost in metallic walls and W_c is the time-averaged electric energy stored by cavity. The total radiated power is [5]:

$$P_r = Re \int_0^{\pi/2} \int_0^{2\pi} \left(\vec{E}_\theta \times \vec{H}^* - \vec{E} \times \vec{H}_\theta^*\right) r^2 \sin\theta \, d\varphi \, d\theta \tag{15}$$

Besides these improvements we have tried to further develop the cavity model. One of the most important drawback of the cavity model was the fact that first it suppose the cavity perfect, and calculate the fields inside it, and then with this fields we calculate the radiation currents at the sides walls. In our model we have suppose that the fields extend outside the cavity, that the magnetic walls are not perfect and the magnetic field amplitude along the x axis has the variation as in Fig. 2. The resonant frequency of a patch with the length *a* is the same that of a cavity with the length *a+2dl,* where [8]

$$dl = 0.412h\frac{\left(\varepsilon_{eff}+0.3\right)\left(b/h+0.264\right)}{\left(\varepsilon_{eff}-0.258\right)\left(b/h+0.8\right)} \quad (16)$$

and ε_{eff} is the dielectric permittivity for a microstrip, considered as a transmission line.

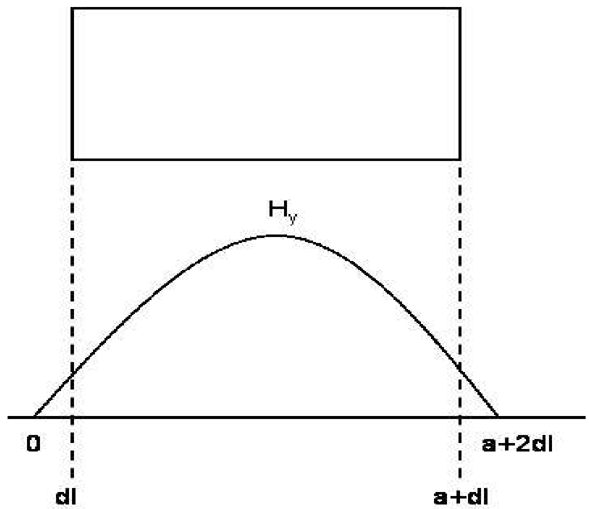

Fig. 2. The representation of the magnetic field H_y along x axis.

For this reason we may assume that the fields are extending outside the patch on a distance *dl*, and the patch act as a cavity with the length *a+2dl*. In this case, if we assume mode TM_{100} for which (in the frame of this assumption), the fields are:

$$E_z = E_0\cos\left(\pi x/\left(a+2dl\right)\right)$$

$$H_y = \frac{j\omega\varepsilon}{\pi}aE_0\sin\left(\pi x/\left(a+2dl\right)\right) \quad (17)$$

and the length of the patch would be taken between *dl* and *a+dl*. Now it is obvious that the magnetic field is zero at the coordinate *0* and *a+2dl* but it would not be zero at the ends of the patch: *dl* and *a+dl*. This means that besides the magnetic currents generated by E_z at the borders there would be also electric currents *J* generated by H_y. In this approximation we calculate the currents on the side walls:

$$\vec{J}_{mx} = E_z\hat{z}\times\hat{y} = \pm E_0\cos\frac{\pi x}{a}\hat{x} \quad \text{for } y=0 \text{ and } y=b \quad (18a)$$

$$\vec{J}_{my} = E_z\hat{z}\times\hat{x} = E_0\cos\frac{\pi dl}{a+2dl}\hat{y} \quad \text{for } x=dl \text{ and } x=a+dl \quad (18b)$$

$$\vec{J}_z = \hat{x}\times H_y\hat{y} = \mp H_0\sin\frac{\pi dl}{a+2dl}\hat{z} \quad \text{for } x=dl \text{ and } x=a+dl \quad (18c)$$

and after the rotation of the radiating apertures in a position parallel to the ground plane the relation (18c) become:

$$\vec{J}_x = H_0\sin\frac{\pi dl}{a+2dl}\hat{z} \quad \text{for } x=dl \text{ and } x=a+dl \quad (18d)$$

Now we suppose that the cavity radiate as four magnetic currents, and two electric currents situated above the ground plane. The J_{mx} currents could be each decomposed as two equal magnetic currents oriented in opposite directions, and so their total radiated field would be zero. The radiation pattern of a patch situated over a large ground plane may be calculated by modeling the radiator as two parallel uniform magnetic line sources of length *b* and width *h* separated by distance *a*, and two uniform electric sources of length *h* and width *b*, separated by the same distance *a*. For an aperture containing both electric and magnetic currents, the radiated fields are [10]:

$$E_\theta = e^{(-jkr)}\begin{pmatrix} -\frac{jk}{4\pi r}\iint\hat{\phi}\cdot\vec{J}_m e^{(jk\hat{r}\,r')}dS - \\ -\frac{j\omega\mu}{4\pi r}\iint\hat{\theta}\cdot\vec{J}e^{(jk\hat{r}\,r')}dS \end{pmatrix} \quad (19)$$

$$E_\phi = e^{(-jkr)}\begin{pmatrix} \frac{jk}{4\pi r}\iint\hat{\theta}\cdot\vec{J}_m e^{(jk\hat{r}\,r')}dS - \\ -\frac{j\omega\mu}{4\pi r}\iint\hat{\phi}\cdot\vec{J}e^{(jk\hat{r}\,r')}dS \end{pmatrix} \quad (20)$$

we obtain:

$$E_\theta = -\frac{jk}{\pi r}\exp(-jk_0 r)E_z\cdot\int_0^h\int_{-b/2}^{b/2}e^{(jk_0 y\sin\theta\sin\phi)}\cos\left(\frac{jk_0 a\sin\theta\cos\phi}{2}\right)dydh\cos\phi -$$
$$-\frac{j\omega\mu_0}{\pi r}\exp(-jk_0 r)H_y\int_0^h\int_{-b/2}^{b/2}e^{(jk_0 y\sin\theta\sin\varphi)}\cos\left(\frac{jk_0 a\sin\theta\cos\varphi}{2}\right)dydh\cos\theta\cos\varphi \quad (21)$$

$$E_\varphi = -\frac{jk}{\pi r}\exp(-jk_0 r)E_z\cdot\int_0^h\int_{-b/2}^{b/2}e^{(jk_0 y\sin\theta\sin\varphi)}\cos\left(\frac{jk_0 a\sin\theta\cos\varphi}{2}\right)dydh\sin\varphi\cos\theta -$$
$$-\frac{j\omega\mu_0}{\pi r}\exp(-jk_0 r)H_y\int_0^h\int_{-b/2}^{b/2}e^{(jk_0 y\sin\theta\sin\varphi)}\cos\left(\frac{jk_0 a\sin\theta\cos\varphi}{2}\right)dydh\sin\varphi \quad (22)$$

In the equations (21) and (22) the two cosines terms under the integration represent the array factor for the two magnetic currents, k_0 is the wave number in free space and we also have take account of the ground plane. After solving the integrals we obtain the radiating fields. From these relations we can determine the radiated fields until a constant E_0 that depend of the excitation.

In our case the power dissipated in dielectric P_d is [11]

$$P_d = \delta\omega\varepsilon \int_{dl}^{a+dl}\int_0^b\int_0^h \vec{E}\cdot\vec{E}^* dv \tag{23}$$

and losses in the electric conducting walls P_m is defined by the relation

$$P_m = 2\sqrt{\frac{\omega\mu}{2\sigma}}\int_{dl}^{a+dl}\int_0^b \vec{H}\cdot\vec{H}^* dS \tag{24}$$

where δ is the dielectric loss tangent and σ is the electrical conductivity. The time-averaged electric energy stored by cavity is [12]

$$W_c = (\varepsilon/4)\int_{dl}^{a+dl}\int_0^b\int_0^h \vec{E}\cdot\vec{E}^* dv \tag{25}$$

Introducing (22), (23), (24) and (25) in (21) we compute δ_{eff} and then introducing k_{eff} in (13) we obtain

$$Z_{in} = \frac{j\omega\mu_0 hc^2}{\varepsilon_r}\sum_{m=0}^{\infty}\sum_{n=0}^{\infty}\frac{\psi_{mn}^2(x_0,y_0)}{\omega_{mn}^2-(1-j\delta_{eff})\omega^2}G_{mn} =$$

$$= \sum_{m=0}^{\infty}\sum_{n-0}^{\infty}\frac{1}{j\omega C_{mn} - j\frac{1}{\omega L_{mn}} + \frac{1}{R_{mn}}} \tag{26}$$

where: $\omega_{mn} = ck_{mn}/\sqrt{\varepsilon_r}$, c is the speed of light, $1/R_{mn}=\omega\delta_{eff}/\alpha_{mn}$, $L_{mn}=\alpha n_{mn}\omega_{mn}^2$, $C_{mn}=1/\alpha_{mn}$ and $\alpha_{mn} = \frac{\mu_0 hc^2}{\varepsilon_r}\psi_{mn}^2(x_0,y_0)G_{mn}$; R_{mn} represent the real part of the impedance, L_{mn} is the inductance and C_{mn} is the capacity at the feed point.

Because all microstrip antennas are narrow-band and they work on one of the cavity mode the $R_{mn}(\omega)$ can be simply approximated by $R_{mn}(\omega_{mn})$ where ω_{mn} is the resonant pulsation of the TM_{mn} mode. This means that the summation in (26) would disappear and would remain only the m and n corresponding to the oscillation mode of the cavity. The input impedance will be

$$\frac{1}{Z_{mn}} = \frac{1}{R_{mn}} + \frac{1}{jX_{mn}} \tag{27}$$

where:

$$R_{mn} = \frac{\mu_0 hc^2}{\varepsilon_r\,\omega_{nm}\delta_{eff}}\psi_{mn}^2(x_0,y_0)G_{mn} \tag{28}$$

$$X_{mn} = \frac{\mu_0 hc^2}{\varepsilon_r(\omega^2/\omega_{mn}) - \omega_{mn}}\psi_{mn}^2(x_0,y_0)G_{mn} \tag{29}$$

For the TM_{100} mode excitation we can easily neglect the other modes because A_{010} and A_{110} are zero and at this mode frequency the other modes contribution to the impedance value can be neglected.

4. Experimental results

Theoretical computations and measurements were made for a rectangular patch of dimension a=2.9 cm, b=1.93 cm, h=0.1 cm with a real permittivity ε_r=2.8 and a loss tangent approximately 0.001. The measurements were made with a vectorial network analyzer. The patch was fed at x_0=1.2 cm and y_0=0.965 cm with a 50 Ω coaxial line. The measured impedance has the form $Z=R+JX$. Putting the computed impedance in a similar form we obtain:

$$R = \frac{R_{mn}X_{mn}^2}{X_{mn}^2 + R_{mn}^2} \tag{30}$$

$$X = \frac{R_{mn}^2 X_{mn}}{X_{mn}^2 + R_{mn}^2} \tag{31}$$

In Table 1 we present the measured and the computed real part of the input impedance for the cavity model [1] and our model around the resonant frequency for the TM_{100} mode.

Table 1.

Frequency MHz	Computed impedance [1]Ω	Computed impedance [our model] Ω	Measured impedance Ω
2970	27.54	28.68	43.64
2975	36.45	38.27	49.57
2980	46.354	49.13	54.801
2985	53.51	57.11	55.45
2990	53.34	56.93	53.432
2995	46	48.8	49.145
3000	36.26	38	43.252

It can be seen that around the resonant frequency, that we found 2985 MHz, both models have an excellent concordance with the experiment. It can be also seen that if we chose a frequency far from the resonance the concordance is no longer as good, but remember that in relation (28) we supposed that $\omega=\omega_{nm}$, and is normal that the model works well only around the resonance. Anyway this peculiarity has little practical importance because the patches are very narrow band antennas and they radiate only at resonant frequencies.

For the same patch, using relations (21) and (22), we have presented in Fig. 3 the computed and the measured radiation patterns for φ = 0° and φ = 90° planes.

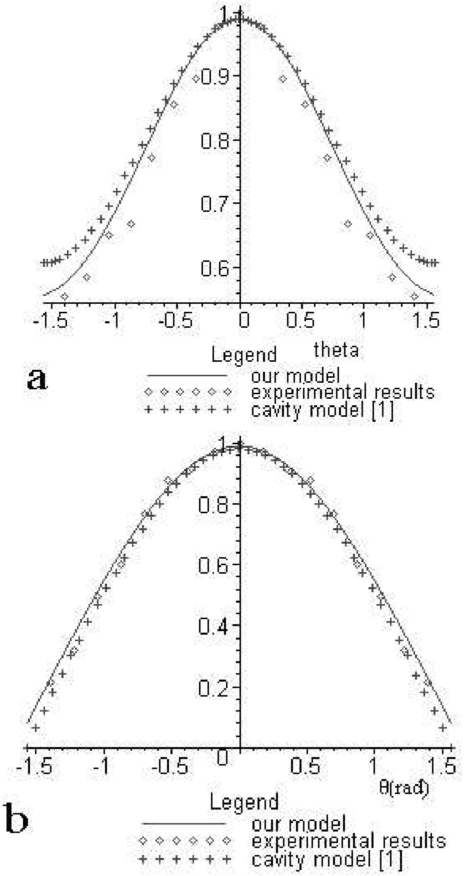

Fig. 3. Radiation pattern for a 3 GHz antenna: a- $\varphi = 0°$ plane; b- $\varphi = 90°$ plane.

We have also compared the results obtained with the cavity model [1] and our model with the experimental results published in other articles.

In Fig. 4 we present the results for a patch with the following dimensions: a = 7.62 cm, b = 11.43 cm, h = 1.5875 mm, and relative dielectric permittivity $\varepsilon_r = 2.62$ [1].

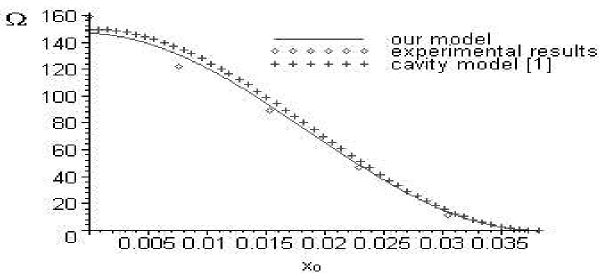

Fig. 4. Impedance dependence with the feeding point for a 1.187 GHz patch.

In Fig. 5 are presented the results for a patch with a = 4.04 cm, b = 5.94, h = 1.27mm, $\varepsilon_r = 2.42$, [13].

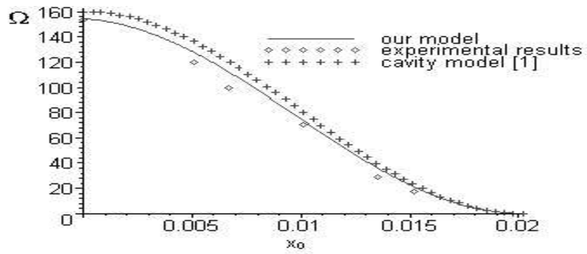

Fig. 5. Impedance dependence with the feeding point for a 2.3 GHz patch.

In Fig. 6 we present the results for a patch with: a = 11,43 cm, b = 7,62 cm, h = 1.5875 mm, and dielectric permittivity $\varepsilon_r = 2.62$ [1].

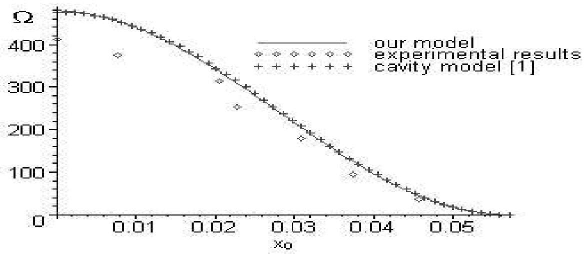

Fig. 6. Impedance dependence with the feeding point for a 803 MHz patch.

5. Conclusions

Radiation of patch antennas is efficient only when the excitation is made at the resonant frequency of a mode. The field is usually dominated by that single mode in the frequency range of interest. Thus the radiation pattern and the input impedance can be determined and they are in good correlation with experiment. It can be seen from Fig. 3 that our model gives better results for the radiation pattern of a patch antenna, mainly in the $\varphi=0^0$ plane. From Table 1 we can see that our model gives better results in 6 cases and worst in 1 case. From Fig. 4, 5 and 6 we can see that our model describes better the dependence of the impedance with the feeding points compared with the improved cavity model developed by Richards et al.

References

[1] W. F. Richards, Y. T. Lo, D. Harrison, IEEE Trans. Antennas Propagation, vol. AP -29 pp. 38-46, 1981.
[2] Y. T. Lo, D. Solomon, W. F. Richards, IEEE Trans. Antennas Propagation, vol. AP-27, pp. 137-145, 1979.
[3] I. J. Bahl, P. Bartia, Artech House, 1980.
[4] N. G. Alexopoulos, N. K. Uzunoghn, I. Rana, IEEE AP-S Int. Symp. Digest, pp. 722-727, 1979.
[5] P. K. Agrawal, M. C. Bailey, IEEE Trans. Antennas Propagation, vol. AP. 25, pp. 756-759, 1977.

[6] R. E. Munson, IEEE Trans. Antennas Propagation, vol. AP-22, 1974, pp. 74-78.
[7] A. K. Bhattacharyya, R. Garg, IEEE Trans. Antennas Propagation. 1985 Reprinted in "Microstrip Antenna Design" edited by K. C. Gupta, A. Benalla.
[8] N. Balanis "Antenna theory: Analysis and design", sec. edition, John Wiley & Sons, N.Y. 1997, chapter 14.
[9] K. R. Carver, J. W. Mink, IEEE Trans. Antennas Propagation, vol. AP-29, pp. 2-24, Jan. 1981.
[10] A. Ishimaru, Prentice Hall International Edition, chapter 9, 1990.
[11] W. F. Richards, Y. T. Lo, Fellow, J. Brewer, IEEE Trans. Antennas Propagation vol. AP-29 pp 150-151 1981.
[12] M. Pozar "Microwave engineering", Adison-Wesly 1993.
[13] L. I.Basilio, M. A. Khayat, J. T. Williams, S. A. Long, IEEE Trans. Antennas Propagation. vol. AP-49 no. 1, 2001.

* Corresponding author: ddsandu@uaic.ro